# MACULAR AND PERIPAPILLARY CHOROIDAL THICKNESS IN DIABETIC PATIENTS

STELA VUJOSEVIC, MD,* FERDINANDO MARTINI, MD,† FABIANO CAVARZERAN, SCD,* ELISABETTA PILOTTO, MD,† EDOARDO MIDENA, MD*†

**Purpose:** To investigate macular and peripapillary choroidal thickness (CT) in diabetic patients with and without diabetic retinopathy (DR).

**Methods:** One hundred and fifty subjects were enrolled: 102 diabetic patients (102 eyes) and 48 normals, as controls. Exclusion criteria were previously treated DR, refractive error higher than ±3 diopters, and treated or untreated glaucoma. All patients underwent full ophthalmic examination, stereoscopic color fundus photography, and spectral domain optical coherence tomography (RS-3000; Nidek). Spectral domain optical coherence tomography examination consisted of linear scans, 6 mm in length, centered onto the fovea, and circle scan positioned around the optic disk (3.46 mm in diameter). Choroidal thickness was measured manually at the fovea and at 1, 2, and 3 mm distance along all scans in the macula. Peripapillary CT was measured at eight points along the circle scan. All measurements were performed independently by 2 masked graders.

**Results:** Mean age was not significantly different between patients with diabetes and controls. In the macular area, CT was significantly lower in the nasal quadrant versus all other quadrants ($P < 0.0001$), in both groups. In the peripapillary area, CT was significantly lower in the inferior quadrant versus all other quadrants ($P < 0.05$), in both groups. Mean macular and peripapillary CT progressively and significantly decreased with increasing level of DR (nonproliferative and proliferative DR vs. controls, $P < 0.05$). No significant CT difference was found between controls and diabetic eyes without detectable DR. Diabetic macular edema did not influence CT. Interobserver coefficient of repeatability was 28.8 (95% confidence interval, 24.8–32.8) for foveal measurements and 13.0 (95% confidence interval, 11.2–14.8) for peripapillary measurements. Pearson correlation coefficient was 0.99, and $P < 0.0001$ for all measurements.

**Conclusion:** Choroidal thickness is reduced in diabetic eyes and parallels appearance and evolution of DR. Spectral domain optical coherence tomography clearly confirms in vivo previously reported histopathologic observations. The role of choroid in the pathophysiology of DR needs to be adequately investigated.

**RETINA** 32:1781–1790, 2012

Diabetic retinopathy (DR) is the leading cause of blindness among working age adults.[1] Retinal vascular and neural alterations are considered the main pathologic phenomena of DR.[1] Increased retinal vascular permeability because of alterations of the blood–retina barriers caused by tight junction disassembly and endothelial cell mediated leukostasis are considered as major mechanisms for retinal edema and ischemia.[2,3]

Clinical and histopathologic findings suggest that vascular changes may also affect the choroid in patients with diabetes.[4] These findings include obstruction of the choriocapillaris, vascular remodeling, choroidal aneurysms, and choroidal neovascularization.[5–8] Because the choroid provides oxygen and nutrients to the outer retina, and it maintains the highly metabolically active photoreceptor cells, choroidal hypoperfusion could result in outer retina dysfunction.[9]

Clinical evaluation of choroid is usually performed by means of indocyanine green angiography, an

From the *Fondazione G. B. Bietti, IRCCS, Roma, Italy; and †Department of Ophthalmology University of Padova, Padova, Italy.

There is no conflicting relationship and no conflict of interest.

Reprint requests: Edoardo Midena, MD, Department of Ophthalmology, University of Padova, 35128 Padova, Italy; e-mail: edoardo.midena@unipd.it

invasive procedure, or contact B-scan ultrasonography, but neither allows for an accurate cross-sectional imaging.[4,10,11] Recently, with the advent of spectral domain optical coherence tomography (SD-OCT), cross-sectional imaging of the choroid has been obtained.[12–17] Different methods have been proposed to obtain an adequate visualization of the choroid with SD-OCT, in normal and pathologic eyes. These include placing SD-OCT closer to the eye to obtain inverted images or the use of research SD-OCT devices, which use a broadband light source in a deeper infrared region compared with conventional devices.[12–15,17–19] Significant variability of choroidal thickness (CT) has been reported in controls, mainly depending on age and refractive error.[13,16,17] In diabetic patients, macular CT was measured with 3-dimensional 1,060-nm SD-OCT and correlated to the degree of diabetic maculopathy.[19]

The aim of this study was to evaluate CT, both in the macula and in the peripapillary area, in diabetic subjects, and to correlate it to the presence and severity of DR.

## Material and Methods

One hundred and two eyes of 102 consecutive diabetic patients were included in this observational case series study. Forty-eight normal volunteers (48 eyes) served as controls. All patients were recruited from the Diabetic Retinopathy Clinic at the Department of Ophthalmology, University of Padova, from September 2009 to June 2011. The inclusion criteria were men or women with Type 1 or 2 diabetes mellitus, any stage of DR (from absent to proliferative DR), refractive error within ±3 diopters (D), and intraocular pressure within normal limits. The exclusion criteria were any type of previous retinal treatment (macular or peripheral laser photocoagulation, vitrectomy, intravitreal steroids, and/or antiangiogenic drugs), significant media opacities that precluded fundus examination or imaging, and treated or untreated ocular hypertension and glaucoma. A written consent form was obtained from all patients as well as the approval from our institutional ethics committee. The study was conducted in accordance with the tenets of the Declaration of Helsinki. Each subject underwent a complete ophthalmic examination, with determination of best-corrected visual acuity, anterior segment examination, Goldmann applanation tonometry, indirect ophthalmoscopy, and 90-D lens biomicroscopy. Then, SD-OCT and fundus photography were obtained. Fluorescein angiography was performed in patients with diabetic macular edema or suspected wide ischemic areas.

### *Study Procedures*

*Visual acuity.* Best-corrected distance visual acuity for each eye was measured by a trained examiner using standard Early Treatment Diabetic Retinopathy Study protocol at 4 m distance with a modified Early Treatment Diabetic Retinopathy Study distance chart transilluminated with a chart illuminator (Precision Vision).[20] Visual acuity was scored as the total number of letters read correctly and converted to the logarithm of the minimum angle of resolution.

*Stereoscopic fundus photography and fluorescein angiography.* Color stereoscopic fundus photographs (seven Early Treatment Diabetic Retinopathy Study fields) and fluorescein angiography (when required) were taken after an adequate dilatation by a trained photographer using the same TOPCON TRC 50IA 35° fundus camera (Topcon, Tokyo, Japan). Diabetic retinopathy was graded as no DR, nonproliferative diabetic retinopathy (NPDR), and proliferative diabetic retinopathy (PDR) by two independent graders experienced in grading of DR.

*Spectral domain optical coherence tomography.* All eyes were examined with SD-OCT (Retinascan RS-3000; NIDEK, Gamagori, Japan). Each eye was examined, after pupillary dilation, both in the macula and peripapillary area. In the macula, 4 radial scans, 6 mm in length, were centered onto the fovea at 0°, 45°, 90°, and 135°. In the peripapillary area, a circle scan centered on the optic disk (3.46 mm diameter, "Disc Circle" option) was used. The scans consisted of 1,024 A-scan with high-definition (50 HD) frame enhancement software. This instrument has a light source of 880-nm wavelength. To improve choroidal visualization, each image consisted of 50 averaged B-scans in a single raster line scan, and the optical coherence tomographic device was positioned close to the eye in order to visualize the image on the top of the monitor (to be in closer proximity to the zero-delay line) in a standard manner (uninverted image). This instrument does not generate inverted images like other SD-OCT machines. The advanced speckle noise reduction system, by averaging images, provided 4-$\mu$m optical coherence tomography digital resolution. Each high-definition line raster image needed to have at least 6 of 10 (maximum) intensity score. To obtain a better image quality, "the toggle switch" option was also used: this function allows to get closer to the eye without moving the scan out of the monitor, obtaining a significantly better in-depth penetration (by

adjusting the z position). Moreover, increasing the luminosity of the images and the luminosity of the monitor and decreasing the contrast of the monitor allowed the graders to better visualize choroidal details. It differs from the recently developed enhanced depth imaging method for choroidal visualization (Heidelberg Spectralis; Heidelberg Engineering, Heidelberg, Germany), which uses an inverted representation of the fundus of each patient and a 100 average B-scans. In this study, we used RS-3000 SD-OCT with direct fundus representation and 50 averaged B-scans and the particular option (toggle switch) that enables better in-depth penetration.

Choroidal thickness was measured as the perpendicular distance between the hyperreflective outer border of the retinal pigment epithelial layer (automatically detected by the instrument) and the sclero–choroidal interface, manually drawn, independently, by each grader (Figure 1). Each grader was blinded to clinical data of all examined eyes.

Choroidal thickness was measured at 25 points for each patient: the foveal center (Fov), at 1, 2, 3 mm temporal (T) (T1, T2, and T3), nasal (N) (N1, N2, and N3), superior (S) (S1, S2, and S3), inferior (I) (I1, I2, and I3), inferotemporal (IT) (IT1, IT2, and IT3) superonasal (SN) (SN1, SN2, and SN3), superotemporal (ST) (ST1, ST2, and ST3), and inferonasal (IN) (IN1, IN2, and IN3) to the fovea, by two independent and masked graders using the embedded SD-OCT software (NAVIS-EX Image Filing Software, RS-3000 OCT). Points located at 1 mm distance from the center of the fovea were numbered 1 and formed a central ring, points located at 2 mm distance from the center of the fovea were numbered 2 and formed an inner ring, points located at 3 mm distance from the center of the fovea were numbered 3 and formed an outer ring.

Peripapillary CT was measured at eight points around the disk: T, ST, S, SN, N, IN, I, and IT, as for macular measurements. Mean CT of the whole peripapillary area, upper hemifield, lower hemifield,

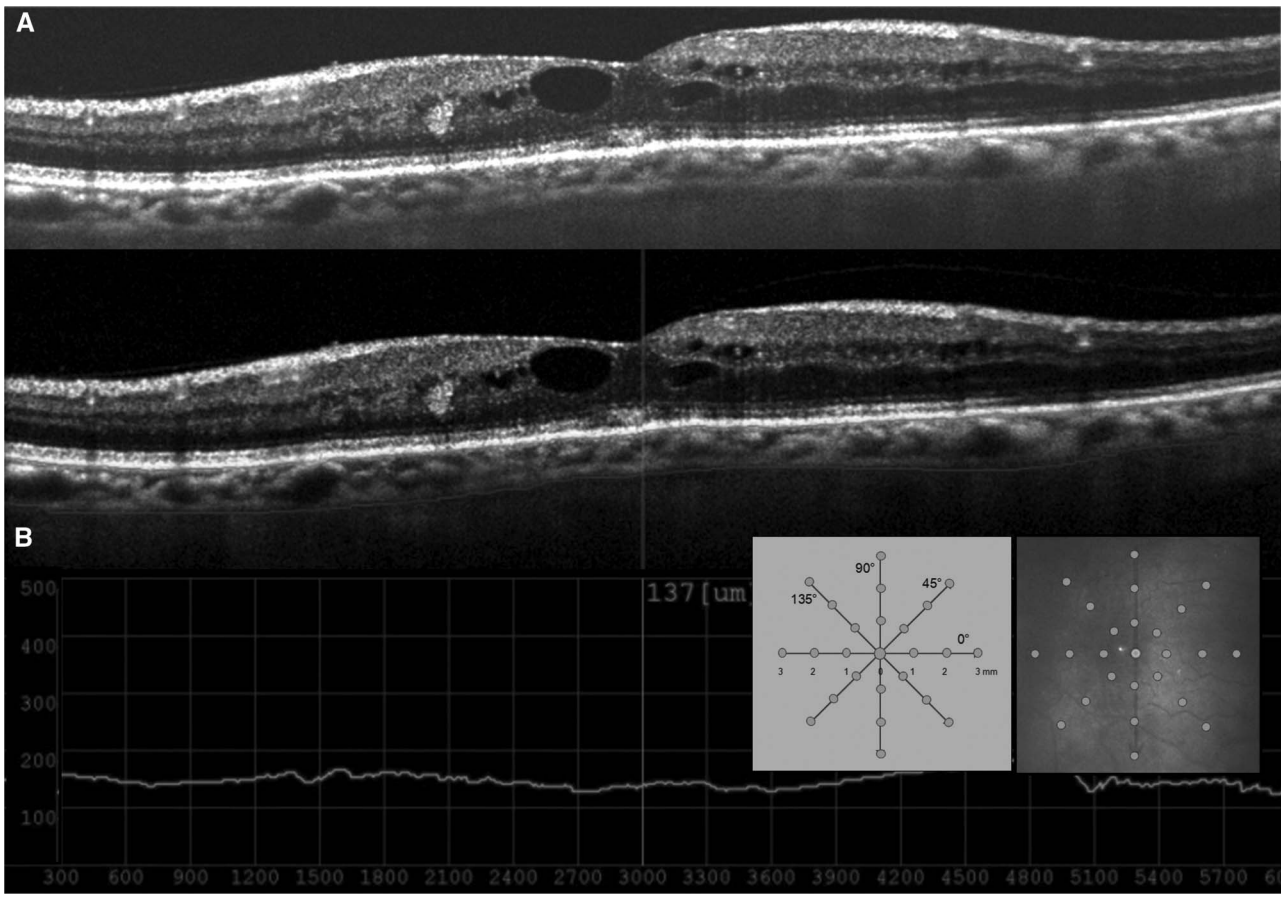


**Fig. 1.** Macular CT in diabetic patient with macular edema and NPDR. **A**, A horizontal OCT scan in the macula showing choroidal structure. **B**, Choroidal thickness is determined as the perpendicular distance between the hyperreflective outer border of the retinal pigment epithelium (automatically detected by the instrument) and the sclero–choroidal interface drawn manually. Foveal CT value (137 $\mu$m, calculated by the instrument) is shown. Bottom right: scheme showing CT measurements at 25 points: foveal center, at 1, 2, 3 mm temporal, N, S, I, IT, SN, ST, and IN to the fovea. OCT, optical coherence tomography.

and T, S, N, and I quadrants were automatically calculated and displayed by the instrument after manually tracing the boundary of the sclero–choroidal interface (Figure 2). Foveal retinal thickness was determined automatically in all eyes.

*Statistical Methods*

Age, spherical equivalent, intraocular pressure, and visual acuity were compared among groups by means of analysis of variance (ANOVA); gender distribution of the groups was compared by means of Fisher exact test. For each subject, CT of different parts of the macula was computed as follows: the individual value of each one of the 25 quantified points; the mean value of each ring: central, inner, and outer, each determined as the average of 8 points; and overall mean value of the measurements from all points. As for peripapillary CT, the following measures were considered in the analyses: the value of each one of the 8 quantified points, the mean value of the upper and lower hemifield, and the overall mean value of all points.

Macula and peripapillary CT were analyzed by means of multiple generalized linear model (GLM) with group (controls, no DR, NPDR, and PDR), age, gender, spherical equivalent, retinal thickness (central subfield retinal thickness [CSF]), and visual acuity as independent variables (between-subject effects). To analyze the CT profile in the macula, distance from the fovea (central ring, inner ring, and outer ring) and single points, GLM model for repeated measures (within-subject effect) was applied. Similar model was applied when peripapillary CT was analyzed about quadrant and upper and lower hemifield of

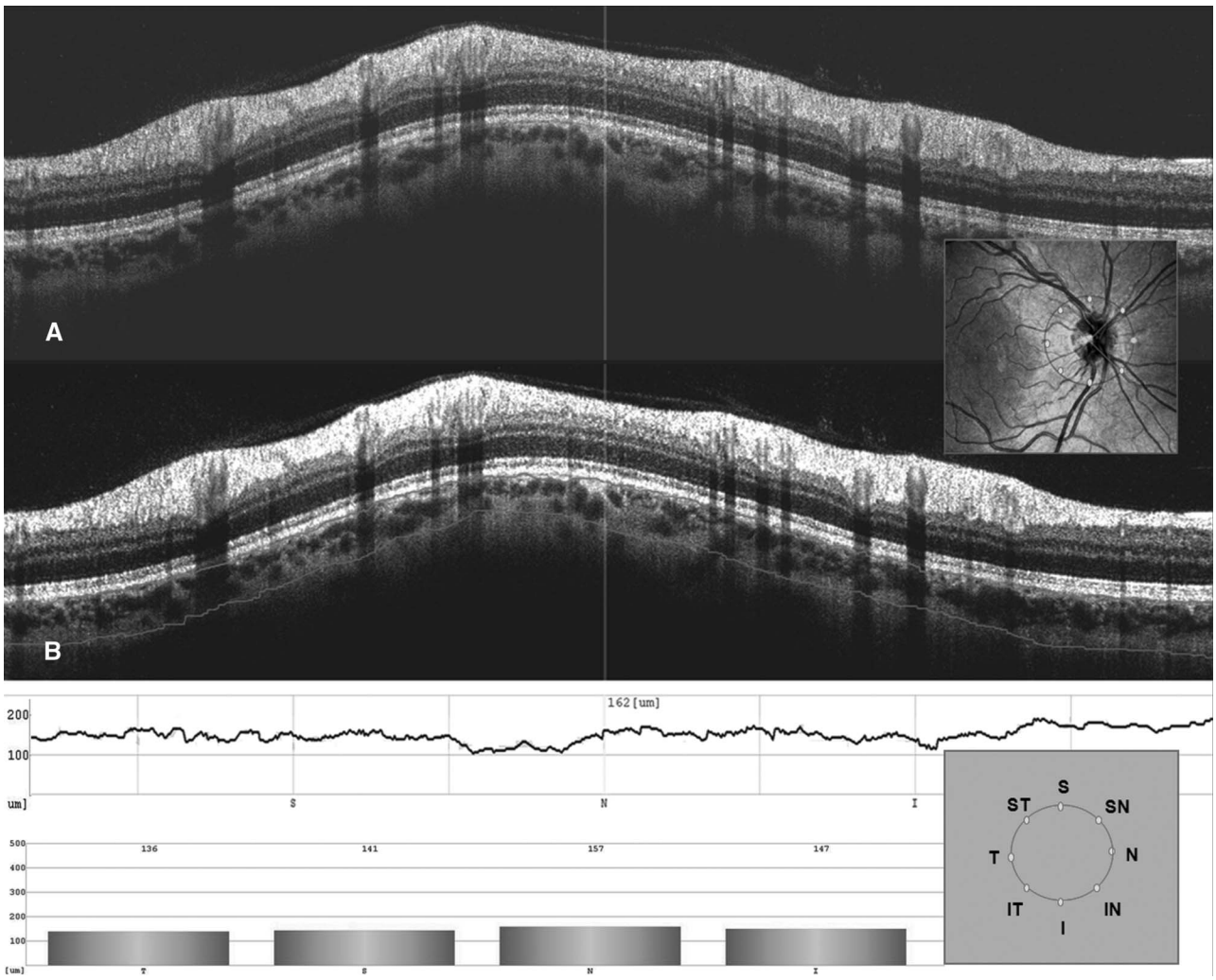


**Fig. 2.** Peripapillary CT in diabetic patient with no clinical signs of DR. **A**, A circle OCT scan centered on the optic disk (3.46 mm diameter). **B**, Choroidal thickness is determined as the perpendicular distance between the hyperreflective outer border of the retinal pigment epithelium (automatically detected by the instrument) and the sclero–choroidal interface drawn manually. Bottom right: Scheme showing peripapillary CT measurements at eight points around the disk: T, ST, S, SN, N, IN, I, and IT. OCT, optical coherence tomography.

measurement. Bonferroni post hoc test was used to compare couples of groups. Relationship between overall macula and peripapillary CT was analyzed by means of Pearson correlation coefficient.

*Interobserver repeatability.* All eyes were evaluated by two experienced readers (A and B): fovea, macular central ring (R1), inner ring (R2), outer ring (R3), and peripapillary thickness (pap TOT) were measured. Readings of the two readers were compared: MacFovA versus MacFovB, MacR1A versus MacR1B, MacR2A versus MacR2B, MacR3A versus MacR3B, and PapTOTA versus PapTOTB. Mean and standard deviation of the differences were calculated. Two-tailed paired *t*-test was used to determine whether compared measurements were significantly different ($P < 0.05$). The relationships between reader's measurements were assessed using the Pearson correlation coefficients. According to Bland–Altman, the difference between readers' measurements were plotted against their mean value. The coefficient of repeatability (defined as 2.77 × Sw, where Sw is the within-subject standard deviation, derived from the mean square of the difference between readers' measurements) as well as the 95% confidence intervals (CIs) were calculated. Significant differences were accepted at $P < 0.05$. All statistical analyses were performed with SAS 9.2 for Windows (SAS, Cary, NC).

## Results

Of 150 enrolled subjects, 77 were women and 73 men. Mean age of patients with diabetes was 57.5 ± 13.3 years (range 31–83 years); mean age of controls was 53.7 ± 14.8 years (range 28–80 years). Twenty-six patients (25.5%) had Type 1 diabetes mellitus and 76 (74.5%) had Type 2 diabetes mellitus. Mean hemoglobin $A_{1c}$ was 8.0% ± 1.5%. Twenty-two patients (eyes) were graded as no DR, 69 patients as NPDR, and 11 patients as PDR. There was no significant difference in age between controls and patients with diabetes ($P = 0.22$). There was no significant difference in age (ANOVA, $P = 0.32$) and spherical equivalent (ANOVA, $P = 0.11$), and intraocular pressure (ANOVA, $P = 0.09$), among controls, no DR, NPDR, and PDR groups. Visual acuity was significantly different among controls, no DR, NPDR, and PDR groups (ANOVA, $P < 0.0001$). In particular, PDR group was significantly different versus controls, no DR, and NPDR group (Bonferroni post hoc test, $P < 0.05$). There was significant difference in gender distribution among controls, no DR, NPDR, and PDR groups (Fisher exact test, $P < 0.0001$). All demographic characteristics of the included patients (eyes) are shown in Table 1.

Figure 3 shows mean CT in the macula of all examined points. There was a significant decrease of CT with increasing age of patients both in the control group and patients with diabetes (GLM, $P < 0.001$). Choroid was thinner in the nasal macula when compared with the S, T, and I macula in all groups (controls, no DR, NPDR, and PDR; GLM, $P < 0.0001$). There was a significant decrease in mean overall CT with increasing level of DR (GLM, $P = 0.0056$). Mean overall CT was significantly lower in the NPDR and PDR groups versus controls (Bonferroni post hoc test, $P < 0.05$; Figure 3, Table 2). Mean overall CT significantly decreased with increasing distance from the fovea (GLM, $P < 0.0001$), irrespective of the group (Figure 3, Table 2). Mean CT was significantly lower in the outer ring versus central ring (Bonferroni post hoc test, $P < 0.01$; Figure 3, Table 2).

Mean foveal CT was 329.5 ± 65.2 $\mu$m in the control group versus 280.6 ± 68.6 $\mu$m in no DR group, 279.4 ± 81.6 $\mu$m in NPDR group, and 230.5 ± 25.8 $\mu$m in PDR group (GLM, $P = 0.02$). Foveal CT was significantly lower in the NPDR and PDR groups versus controls (Bonferroni post hoc test, $P < 0.05$).

Figure 4 shows mean CT in the peripapillary area. Mean overall CT was 199.7 ± 9.6 $\mu$m in the control group, 181.6 ± 12.6 $\mu$m in no DR group, 156.7 ± 6.2 $\mu$m in NPDR group, and 129.2 ± 14.4 $\mu$m in PDR group. There was a significant decrease in mean overall CT (whole peripapillary area) with the increasing level of DR (GLM, $P = 0.0041$). Mean overall CT was significantly lower in the NPDR and PDR groups versus control and in the PDR group versus no DR group (Bonferroni post hoc test, $P < 0.05$). Control and no DR groups were not significantly different. Mean CT was significantly lower in the lower hemifield versus upper hemifield in all groups (control, no DR, NPDR, and PDR groups; GLM, $P = 0.0016$).

Table 3 shows mean peripapillary CT values in four quadrants (S, N, I, and T). Choroidal thickness was significantly different among 4 quadrants (GLM, $P < 0.0001$). Choroidal thickness was significantly lower in the inferior quadrant versus all other quadrants in all groups (Bonferroni post hoc test, $P < 0.05$).

Correlation between mean overall macular and peripapillary CT was good in no DR group ($R = 0.72$, $P < 0.0001$), almost perfect for NPDR group ($R = 0.83$, $P < 0.0001$), and not significant for PDR group ($R = 0.38$, $P = 0.25$) probably because of the limited number of eyes (Figure 5).

Mean retinal thickness in the fovea was 264.1 ± 4.4 $\mu$m in the control group, 274 ± 5.4 $\mu$m in no DR group, 298.6 ± 6.6 $\mu$m in NPDR group, and 307.7 ± 14.8 $\mu$m in PDR group. There was no significant correlation between mean foveal choroidal and

Table 1. Descriptive Statistics of Patients Under Study

| | | | Grade of DR | | |
|---|---|---|---|---|---|
| | Control | Patients With Diabetes | No DR | NPDR | PDR |
| Patients, n (%) | 48 (32) | 102 (68) | 22 (16.9) | 69 (53.1) | 11 (8.5) |
| Gender, M/F | 18/30 | 55/47 | 8/14 | 43/26 | 4/7 |
| Mean age (SD), yrs | 53.7 (14.8) | 57.5 (13.3) | 57.6 (13.5) | 57.8 (14.0) | 57.4 (9.8) |
| HbA1c (SD), % | — | 8.0 (1.5) | — | — | — |
| Patients, n (%) | | | | | |
| Diabetes Type 1 | — | 26 (25.5) | 2 (6.5) | 22 (87) | 2 (6.5) |
| Diabetes Type 2 | — | 76 (74.5) | 20 (26.3) | 47 (61.8) | 9 (11.8) |
| Mean duration of DM (SD), yrs | | | | | |
| Diabetes Type I | — | 26.1 (8.4) | 10.0 | 26.3 (6.6) | 40.0 |
| Diabetes Type II | — | 12.3 (10.1) | 4.8 (3.4) | 15.7 (10.8) | 9.0 (6.5) |
| Visual acuity (SD), logMAR | 0.009 (0.045) | 0.098 (0.212) | 0.050 (0.118) | 0.067 (0.107) | 0.394 (0.491) |
| SE | 0.009 (0.847) | 0.289 (1.149) | 0.256 (0.937) | 0.398 (1.192) | 0.363 (1.170) |
| IOP (SD), mmHg | 15.7 (2.0) | 16.9 (3.7) | 16.2 (3.4) | 16.9 (2.9) | 17.6 (4.8) |

DM, diabetes mellitus; F, female; IOP, intraocular pressure; logMAR, logarithm of the minimum angle of resolution; M, male; SD, standard deviation; SE, spherical equivalent.

retinal thickness in patients with diabetes ($R = 0.015$, $P = 0.88$; Figure 6).

Table 4. summarizes interobserver repeatability. None of the mean differences between readers' measurements resulted statistically significant. Coefficient of repeatability obtained from the fovea and the peripapillary area measurements was 28.8 (95% CI, 24.8–32.8) and 13.0 (95% CI, 11.2–14.8), respectively. Average measurement of central, inner, and outer rings showed a coefficient of repeatability between 19.7 (95% CI, 16.9–22.4) and 23.2 (95% CI, 20.0–26.5). All Pearson correlations were highly statistically significant ($P < 0.0001$). Bland–Altman plot of difference against mean CT showed no significant change in variability for the range of CT, and a very few observations were outside 95% confidence limits (Figure 7).

## Discussion

In this study, we found, by means of SD-OCT, that CT decreases both in the macula and in the peripapillary area in diabetic eyes with clinical signs of DR compared with controls. In diabetic eyes with no clinical signs of DR, CT does not significantly differ from controls. The choroid comprises blood vessels, melanocytes, fibroblasts, resident immunocompetent cells, and supporting collagenous and elastic connective tissue. Thus, its main structure is vascular with some connective tissues.[21] Therefore, its thickness is probably related to the diameter of the choroidal vessels, the number of large choroidal vessels, and the amount of connective tissue. Hence, relative vasoconstriction or reduced perfusing pressure may account for reduced endoluminal volume and apparent thinning. According to our data, choroidal thinning in diabetic eyes seems an overall phenomenon, at least homogeneously involving both central and peripapillary choroid. We found that the choroid is thinner in the nasal portion of the macula, especially with increasing distance from the fovea, both in controls and in patients with diabetes. This confirms recently published data about CT in the macular area in normal and diabetic subjects

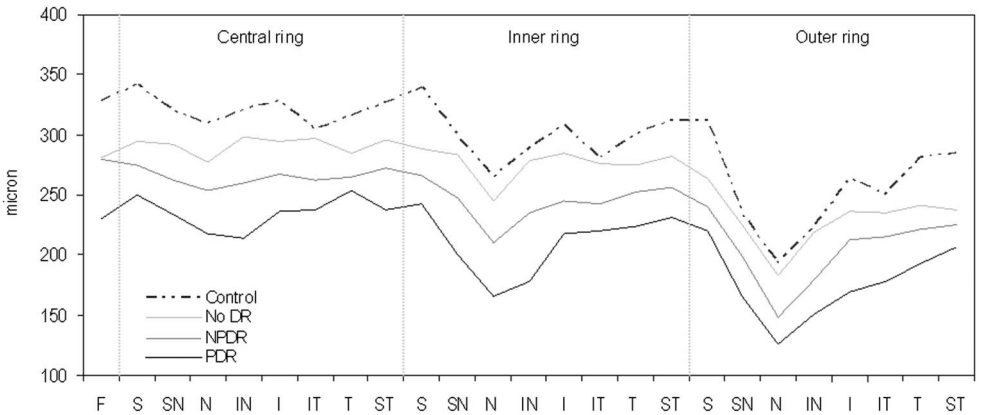


**Fig. 3.** Graph 1. Choroidal thickness in the macula. Central ring, 1 mm distance from the fovea; inner ring, 2 mm distance from the fovea; outer ring, 3 mm distance from the fovea.

Table 2. Macular CT of All Examined Points (Mean, SD)

| Ring | Point | Control (n = 48) | No DR (n = 22) | NPDR (n = 69) | PDR (n = 11) |
|---|---|---|---|---|---|
| | Fovea | 329.5 (65.2) | 280.6 (68.6) | 279.4 (81.6) | 230.5 (25.8) |
| Central | S | 341.2 (66.3) | 294.5 (75.6) | 275.2 (81.6) | 250.3 (41.8) |
| | SN | 318.9 (56.7) | 292.1 (77.2) | 262.3 (82.4) | 233.5 (51.2) |
| | N | 310.4 (68.4) | 277.2 (78.6) | 253.9 (86.4) | 217.8 (47.4) |
| | IN | 321.1 (67.7) | 298.5 (94.2) | 259.5 (83.6) | 213.5 (43.0) |
| | I | 328.1 (66.3) | 295.0 (85.9) | 267.5 (80.6) | 236.6 (43.8) |
| | IT | 305.4 (65.8) | 297.3 (83.8) | 261.8 (82.7) | 238.0 (44.1) |
| | T | 315.9 (78.1) | 284.8 (77.2) | 265.2 (77.5) | 253.9 (45.1) |
| | ST | 326.6 (74.5) | 296.0 (80.8) | 272.7 (79.5) | 238.1 (35.5) |
| Inner | S | 338.9 (66.2) | 288.7 (81.4) | 266.3 (81.3) | 242.8 (41.5) |
| | SN | 297.8 (59.3) | 283.1 (75.9) | 247.2 (77.6) | 200.6 (66.7) |
| | N | 264.7 (73.4) | 245.0 (85.4) | 210.0 (82.3) | 166.1 (62.0) |
| | IN | 287.9 (66.6) | 278.1 (87.1) | 234.7 (78.5) | 178.1 (45.6) |
| | I | 308.4 (71.8) | 284.8 (94.9) | 245.5 (77.7) | 217.2 (44.6) |
| | IT | 279.8 (66.9) | 275.7 (83.5) | 242.6 (82.4) | 219.9 (45.7) |
| | T | 300.1 (80.5) | 274.3 (76.1) | 252.3 (70.6) | 224.0 (44.6) |
| | ST | 311.4 (69.7) | 282.3 (79.7) | 256.8 (71.8) | 231.5 (62.4) |
| Outer | S | 312.4 (75.9) | 263.4 (72.3) | 240.6 (72.9) | 220.2 (48.3) |
| | SN | 234.2 (67.5) | 225.4 (77.6) | 199.5 (70.0) | 165.2 (69.4) |
| | N | 192.7 (67.6) | 183.0 (72.0) | 148.0 (61.5) | 125.7 (68.8) |
| | IN | 223.1 (61.9) | 219.0 (71.7) | 179.8 (53.2) | 150.4 (42.7) |
| | I | 263.7 (69.1) | 236.8 (83.4) | 213.0 (79.3) | 169.6 (52.3) |
| | IT | 249.5 (73.7) | 235.5 (74.5) | 215.9 (71.2) | 178.1 (51.2) |
| | T | 281.2 (78.0) | 240.9 (72.1) | 220.9 (72.7) | 192.6 (42.7) |
| | ST | 284.3 (67.3) | 238.1 (61.4) | 225.6 (76.5) | 206.5 (65.7) |

Central ring, 1 mm distance from the fovea; inner ring, 2 mm distance from the fovea; outer ring, 3 mm distance from the fovea.

using different SD-OCTs.[13,16,22] Margolis and Spaide[13] showed, by means of inverted images using Heidelberg Spectralis SD-OCT (Heidelberg Engineering), that CT decreases rapidly in the nasal direction, up to 3 mm from the fovea. Manjunath et al[16] showed, by means of Cirrus SD-OCT (Cirrus-HD; Carl Zeiss Meditec, Inc, Dublin, CA), that the choroid is thinner in the nasal portion of the macula and near the optic disk in controls. Regatieri et al[22] showed that choroid is thinner in the nasal and temporal portions of the macula in both controls and patients with diabetes by means of Cirrus SD-OCT. Esmaeelpour et al[18] reported negative correlation between subfoveal CT and axial length and variable correlation between perifoveal CT and axial length in myopic and hyperopic eyes, using a 3-dimensional 1,060-nm SD-OCT. Different authors have also reported that CT is an age-dependent parameter.[13,16,17,23] A significant reduction in CT with increasing age is also confirmed by this study, both in normal and diabetic subjects (data not shown). Margolis and Spaide[13] found a 16 $\mu$m decrease of CT per decade of life. Furthermore, Spaide[24] described an entity called age-related choroidal atrophy, consisting in significant decrease in CT because of small vessel disease affecting the choroid in the elderly.

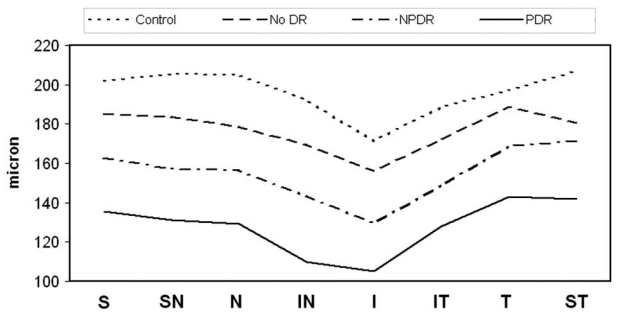


**Fig. 4.** Graph 2. Peripapillary CT profiles. All measurements are performed at 3.46 mm from the center of the optic disk.

In this study, we also describe the pattern of CT in the peripapillary area in both controls and patients with diabetes. Inferior peripapillary quadrant was found to be thinner than the other quadrants in controls. This is in accordance with recently published data by Ho et al[25] in normal subjects in which a significant decrease in CT was found in the inferior portion of the peripapillary area versus all other peripapillary quadrants by means of high-definition SD-OCT. This pattern is maintained in diabetic eyes, as shown in the present study. Moreover, in diabetic eyes, the decrease of peripapillary CT progresses with increasing severity of DR. Johnson et al described peripapillary choriocapillaris non perfusion, as the most consistent abnormality in choroidal circulation in spontaneously

Table 3. Peripapillary CT Determined Automatically by the Instrument (Mean, SD)

| Point | Control (n = 48) | No DR (n = 22) | NPDR (n = 69) | PDR (n = 11) |
|---|---|---|---|---|
| S | 208.1 (50.7) | 187.8 (62.3) | 164.9 (51.6) | 135.1 (49.9) |
| N | 201.2 (58.8) | 179.1 (55.1) | 155.7 (50.2) | 126.7 (56.8) |
| I | 182.1 (45.4) | 166.7 (62.9) | 137.1 (46.8) | 112.9 (43.9) |
| T | 200.3 (47.3) | 185.4 (61.6) | 167.4 (62.0) | 137.5 (46.7) |

diabetic monkeys (Johnson et al. Invest Ophthalmol Vis Sci 2004;45:ARVO E-Abstract 3252).

The thinning of peripapillary choroid might also explain a higher risk of developing primary glaucoma, in diabetic patients.[26,27] This might be because of the reduced contribution of choroidal blood supply to the prelaminar part of the optic disk, as found in "senile sclerotic glaucoma."[28]

In this study, we found no significant correlation between choroidal and retinal thickness in the macular area. In a recent article, Esmaeelpour et al[19] showed decreased macular CT in diabetic patients with or without diabetic maculopathy with no difference in foveal CT among different maculopathy groups. Moreover, when we separately evaluated patients with diabetic macular edema (with increased retinal thickness on SD-OCT) versus patients without edema, CT was not significantly different (data not shown). This might be explained by the fact that macular edema is primarily caused by altered retinal circulation, which leads to increased retinal thickness, with no concurrent specific alterations in CT.

A structurally and functionally normal choroid is essential for the normal function of the retina. Choriocapillaris degeneration, previously demonstrated in histopathologic studies, may be responsible for photoreceptor dysfunction and death by insufficient removal of waste products generated by the retinal pigment epithelial cells and consequent accumulation of such waste in the Bruch membrane.[29] These can ultimately lead to choroidal autoinfarction and atrophy (indirectly visualized as reduced CT) determining visual loss.

Interobserver repeatability in manually evaluating CT showed the coefficient of repeatability ranging between 13 $\mu$m and 28 $\mu$m. This is consistent with recently published articles, which analyzed reproducibility and repeatability of manually measured CT by SD-OCT.[25,30–32] Moreover, all measurements performed in this study were obtained using direct uninverted scans, a methodology that allows to simply obtaining and managing SD-OCT images. This method differs from the enhanced depth imaging method, described recently by Spaide et al[12] using the Heidelberg Spectralis SD-OCT. With enhanced depth imaging, an inverted image positioned near the top of the display and a 100 average B-scans were used for choroidal visualization. Although measurements of

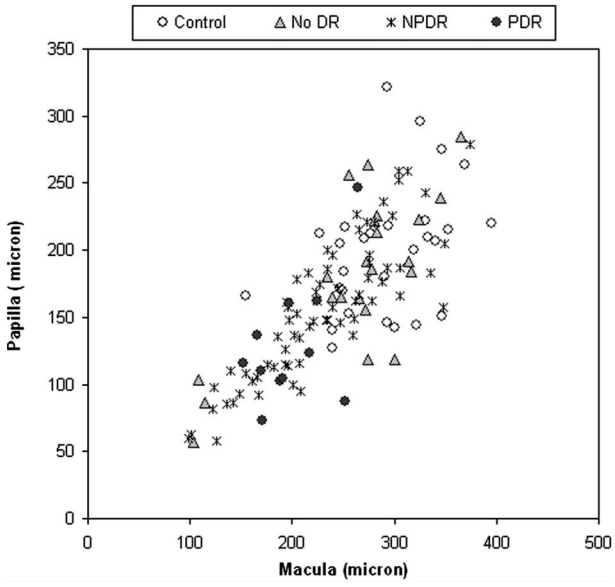


**Fig. 5.** Graph 3. Correlation between macular and peripapillary CT.

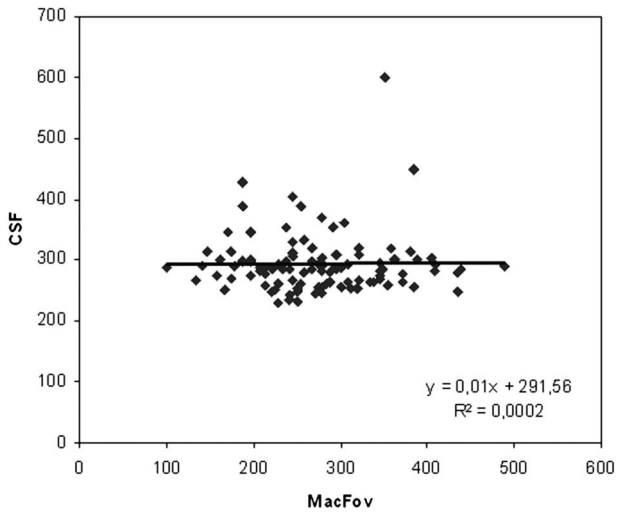


**Fig. 6.** Graph 4. Correlation between foveal CT (MacFov) and central retinal thickness (central subfield retinal thickness) in patients with diabetes. MacFov, foveal CT; CSF, central retinal thickness; choroidal and retinal thickness values are expressed in microns.

Table 4. Summary of Interobserver Repeatability

| Site | Mean Difference | SD | Range | *P* | Pearson Correlation Coefficient | CR | 95% CI |
|---|---|---|---|---|---|---|---|
| Fovea | −0.8 | 10.4 | −21.0 to 59.0 | 0.46 | 0.992 | 28.8 | 24.8 to 32.8 |
| Central ring | 0.8 | 7.1 | −21.4 to 23.4 | 0.29 | 0.998 | 19.7 | 16.9 to 22.4 |
| Inner ring | −1.2 | 7.9 | −17.0 to 19.3 | 0.14 | 0.997 | 22.0 | 18.9 to 25.1 |
| Outer ring | −1.1 | 8.4 | −25.5 to 27.1 | 0.18 | 0.995 | 23.2 | 20.0 to 26.5 |
| Papilla | −0.5 | 4.7 | −12.6 to 30.4 | 0.29 | 0.997 | 13.0 | 11.2 to 14.8 |

CR, coefficient of repeatability; SD, standard deviation.

CT are performed in similar ways using "layer editing" function in both instruments, direct visualization of images is more straightforward and natural in optical coherence tomography image analysis. According to our experience, to better visualize the choroid with RS-3000, well-dilated pupils are needed, even in normal and young subjects. On the contrary, with enhanced depth imaging method, good quality choroidal images are obtained even in undilated controls.[12]

Whereas the choroid may be investigated using B-scan ultrasonography and/or indocyanine green angiography, both these techniques have major limitations. The former allows for limited resolution and suffers from limited reproducibility. The latter is an invasive technique with more qualitative than quantitative results. Spectral domain optical coherence tomography has the advantage of clear and repeatable images, with reproducible quantification of choroidal parameters. Moreover, this technique is undergoing

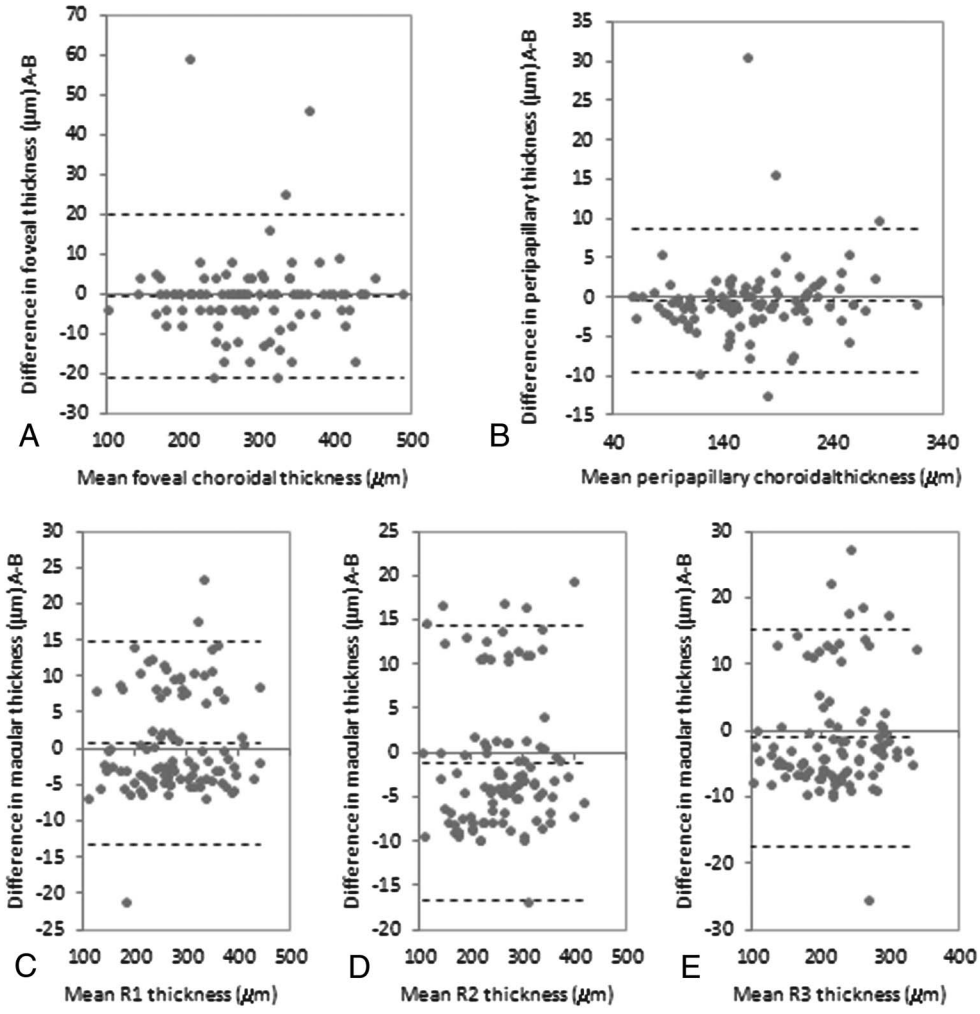


**Fig. 7.** Graph 5. Bland–Altman plots of differences between two observers (Observer A and Observer B) against mean CT in different sites. **A**, Mean foveal CT. **B**, Mean peripapillary CT. **C**, Mean CT in the central ring (R1). **D**, Mean CT in the inner ring (R2). **E**, Mean CT in the outer ring (Ring 3).

impressive technologic improvement, with the future possibility of fully automatic measurement of CT.

Choroidal thinning as documented in this study, and when confirmed in a larger population, should stimulate to reconsider the pathophysiologic role of choroidal circulation in the natural history of DR, mainly in outer retina impairment.

**Key words:** diabetic retinopathy, choroid, choroidal thickness, OCT.

## References


1. Antonetti DA, Barber AJ, Bronson SK, et al. Diabetic retinopathy: seeing beyond glucose-induced microvascular disease. Diabetes 2006;55:2401–2411.
2. Antonetti DA, Lieth E, Barber AJ, Gardner TW. Molecular mechanisms of vascular permeability in diabetic retinopathy. Semin Ophthalmol 1999;14:240–248.
3. Miyamoto K, Khosrof S, Bursell SE, et al. Prevention of leukostasis and vascular leakage in streptozotocin-induced diabetic retinopathy via intercellular adhesion molecule-1 inhibition. Proc Natl Acad Sci U S A 1999;96:10836–10841.
4. Weinberger D, Kramer M, Priel E, et al. Indocyanine green angiographic findings in non proliferative diabetic retinopathy. Am J Ophthalmol 1998;126:238–247.
5. Cao J, McLeod S, Merges CA, Lutty GA. Choriocapillaris degeneration and related pathologic changes in human diabetic eyes. Arch Ophthalmol 1998;116:589–597.
6. Fukushima I, McLeod DS, Lutty GA. Intrachoroidal microvascular abnormality: a previously unrecognized form of choroidal neovascularization. Am J Ophthalmol 1997;124:473–487.
7. Hidayat AA, Fine BS. Diabetic choroidopathy. Light and electron microscopic observations of seven cases. Ophthalmology 1985;92:512–522.
8. McLeod DS, Lutty GA. High-resolution histologic analysis of the human choroidal vasculature. Invest Ophthalmol Vis Sci 1994;35:3799–3811.
9. Lutty GA, Cao J, McLeod DS. Relationship of polymorphonuclear leukocytes to capillary dropout in the human diabetic choroid. Am J Pathol 1997;151:707–714.
10. Shiragami C, Shiraga F, Matsuo T, et al. Risk factors for diabetic choroidopathy in patients with diabetic retinopathy. Graefes Arch Clin Exp Ophthalmol 2002;240:436–442.
11. Coleman DJ, Silverman RH, Chabi A, et al. High-resolution ultrasonic imaging of the posterior segment. Ophthalmology 2004;111:1344–1351.
12. Spaide RF, Koizumi H, Pozzoni MC. Enhanced depth imaging spectral-domain optical coherence tomography. Am J Ophthalmol 2008;146:496–500.
13. Margolis R, Spaide RF. A pilot study of enhanced depth imaging optical coherence tomography of the choroid in normal eyes. Am J Ophthalmol 2009;147:811–815.
14. Spaide RF. Enhanced depth imaging optical coherence tomography of retinal pigment epithelial detachment in age-related macular degeneration. Am J Ophthalmol 2009;147:644–652.
15. Fujiwara T, Imamura Y, Margolis R, et al. Enhanced depth imaging optical coherence tomography of the choroid in highly myopic eyes. Am J Ophthalmol 2009;148:445–450.
16. Manjunath V, Taha M, Fujimoto JG, Duker JS. Choroidal thickness in normal eyes measured using Cirrus HD optical coherence tomography. Am J Ophthalmol 2010;150:325–329.
17. Ikuno Y, Kawaguchi K, Nouchi T, Yasuno Y. Choroidal thickness in healthy Japanese subjects. Invest Ophthalmol Vis Sci 2010;51:2173–2176.
18. Esmaeelpour M, Povazay B, Hermann B, et al. Three-dimensional 1060-nm OCT: choroidal thickness maps in normal subjects and improved posterior segment visualization in cataract patients. Invest Ophthalmol Vis Sci 2010;51:5260–5266.
19. Esmaeelpour M, Považay B, Hermann B, et al. Mapping choroidal and retinal thickness variation in type 2 diabetes using three-dimensional 1060-nm optical coherence tomography. Invest Ophthalmol Vis Sci 2011;52:5311–5316.
20. Ferris FL III, Kassoff A, Bresnick GH, Bailey I. New visual acuity charts for clinical research. Am J Ophthalmol 1982;94:91–96.
21. Nickla DL, Wallman J. The multifunctional choroid. Prog Retin Eye Res 2010;29:144–168.
22. Regatieri CV, Branchini L, Fujimoto JG, Duker JS. Choroidal imaging using spectral-domain optical coherence tomography. Retina 2012;32:865–876.
23. McCourt EA, Cadena BC, Barnett CJ, et al. Measurement of subfoveal choroidal thickness using spectral domain optical coherence tomography. Ophthalmic Surg Lasers Imaging 2010;41:S28–S33.
24. Spaide RF. Age-related choroidal atrophy. Am J Ophthalmol 2009;147:801–810.
25. Ho J, Branchini L, Regatieri C, et al. Analysis of normal peripapillary choroidal thickness via spectral domain optical coherence tomography. Ophthalmology 2011;118:2001–2007.
26. Kim C, Kim TW. Comparison of risk factors for bilateral and unilateral eye involvement in normal-tension glaucoma. Invest Ophthalmol Vis Sci 2009;50:1215–1220.
27. Drance S, Anderson DR, Schulzer M, et al. Risk factors for progression of visual field abnormalities in normal-tension glaucoma. Am J Ophthalmol 2001;131:699–708.
28. Geijssen HC, Greve EL. The spectrum of primary open angle glaucoma. I: senile sclerotic glaucoma versus high tension glaucoma. Ophthalmic Surg 1987;18:207–213.
29. Cao J, McLeod S, Merges CA, Lutty GA. Choriocapillaris degeneration and related pathologic changes in human diabetic eyes. Arch Ophthalmol 1998;116:589–597.
30. Benavente-Pérez A, Hosking SL, Logan NS, Bansal D. Reproducibility-repeatability of choroidal thickness calculation using optical coherence tomography. Optom Vis Sci 2010;87:867–872.
31. Rahman W, Chen FK, Yeoh J, et al. Repeatability of manual subfoveal choroidal thickness measurements in healthy subjects using the technique of enhanced depth imaging optical coherence tomography. Invest Ophthalmol Vis Sci 2011;52:2267–2271.
32. Yamashita T, Yamashita T, Shirasawa M, et al. Repeatability and reproducibility of subfoveal choroidal thickness in normal eyes of Japanese using different SD-OCT devices. Invest Ophthalmol Vis Sci 2012;53:1102–1107.